Available online at www.sciencedirect.com
ScienceDirect
Journal of Solid State Chemistry 179 (2006) 3371–3377
JOURNAL OF SOLID STATE CHEMISTRY
www.elsevier.com/locate/jssc

Temperature-dependent crystallographic studies and electronic structure of $Ba_2Cd_3Bi_4$

Sheng-qing Xia, Svilen Bobev*

Department of Chemistry and Biochemistry, University of Delaware, Newark, Delaware 19716, USA

Received 19 April 2006; received in revised form 20 June 2006; accepted 2 July 2006
Available online 7 July 2006

Abstract

The ternary compound $Ba_2Cd_3Bi_4$ crystallizes in the *C*-centered orthorhombic space group *Cmce* (No. 64) with its own type (Pearson's symbol *oC*36; $a = 7.019(3)$ Å, $b = 17.389(7)$ Å and $c = 9.246(3)$ Å determined at −23 °C). Although the structure of this intermetallic compound with transition metal in d^{10} configuration has already been established, details such as the rather unusual coordination of the Cd-atoms and the elongation in specific direction of their anisotropic displacement parameters had not been explained. These facts, along with the higher than 12% *R*-values from the original structure determination prompted the systematic structural studies by single-crystal X-ray diffraction at several different temperatures. The results from these studies confirm strong temperature dependence of the cadmiums' anisotropic displacement parameters, concomitant rather large thermal expansion along the crystallographic *b*-axis. Electronic band structure calculations performed by the TB-LMTO-ASA method are also reported.

Keywords: $Ba_2Cd_3Bi_4$; Crystal structure; TB-LMTO-ASA calculation; Structural disorder

1. Introduction

As part of the ongoing efforts to elucidate the complicated structure–property relationships in various polar intermetallic compounds in the systems *A–TM–Pn* (*A* = alkaline-earth metal; TM = d^5 or d^{10} transition metal; *Pn* = Sb or Bi), we turned our attention to the Ba-Cd-Bi phase diagram [1–3]. The initial scope of this work was to synthesize and characterize the hitherto unknown ternary compound $Ba_9Cd_{4+x}Bi_9$, isostructural with the recently reported $Yb_9Zn_{4+x}Sb_9$ ($0 < x < 0.5$) [3]. These studies were aimed at better understanding the structural complexity along with the possible phase width and their effect on the physical properties. Instead, the reactions between Ba, Cd and Bi, resulted in the discovery of a new material, the monoclinic $Ba_{11}Cd_8Bi_{14}$, with unique layered polyanionic framework, composed of corner- and edge-shared $CdBi_4$ tetrahedra. These are arranged so that they form ribbons connected to each other through novel "zigzag" chains of Bi [2].

In an attempt to grow larger crystals of $Ba_{11}Cd_8Bi_{14}$ from a reaction of Ba, Cd and Bi carried out in Cd-flux, we serendipitously "discovered" $Ba_2Cd_3Bi_4$ as one of the side products. Although the structure of this compound (its own type, Pearson's symbol *oC*36) has already been reported [4], with residuals higher than 12% and abnormal anisotropic displacement parameters for the Cd-atoms, it seemed that the 1982 report by Schäfer et al. might not be the final word in that regard [4]. Therefore, intrigued by the unprecedented Cd-coordination, we undertook systematic structural studies by single-crystal X-ray diffraction and refined the structure at several different temperatures. The results confirm strong temperature dependence of the cadmiums' anisotropic displacement parameters, concomitant rather large thermal expansion along the *b*-axis. Electronic band structure calculations performed by the TB-LMTO-ASA method are also reported.

2. Experimental

2.1. Synthesis

All manipulations were performed inside an argon-filled glove box or under vacuum. The metals were commercial

*Corresponding author. Fax: 302 831 6335.
E-mail address: sbobev@chem.udel.edu (S. Bobev).

0022-4596/$ - see front matter © 2006 Elsevier Inc. All rights reserved.
doi:10.1016/j.jssc.2006.07.003

grade and used as received: Ba (Aldrich, rod, 99 + %), Cd (Alfa, shot, 99.999%), Bi (Alfa, rod, 99.99%). The reactions (with starting materials in a ratio Ba:Cd:Bi = 1:12:2) were carried out in alumina crucibles, which were subsequently sealed in evacuated fused silica jackets. Each reaction mixture was heated from 100 to 800 °C at a rate of 200 °C/h, allowed to dwell at this temperature for 20 h, and subsequently slowly cooled down to 450 °C at a rate of 5 °C/h. The flux was removed by centrifugation at 450 °C and further details on the procedure can be found elsewhere [1–3]. The crystals of $Ba_2Cd_3Bi_4$ are needle-shaped, dark, and with metallic luster, which slowly lose their shiny appearance upon exposure to air. *Caution:* due to the high toxicity of the cadmium metal and its compounds, both the reagents and the products were handled with extreme care and appropriate personal protective equipment.

The synthesis of $Ba_2Cd_3Bi_4$ described by Schäfer et al. involved a reaction of the elements in a sealed tube, which was heated at 800 °C for 1 h, then slowly cooled to room temperature [4]. In our experiments, Cd-excess and similar temperature profiles was used to grow crystals of $Ba_2Cd_3Bi_4$. All of the above suggests that $Ba_2Cd_3Bi_4$ is a congruently melting compound in the Ba–Cd–Bi phase diagram. The tetragonal $BaCdBi_2$ reportedly melts congruently as well [5], however, crystals from this phase were never identified as product from Cd-flux at the conditions described above ($BaCdBi_2$ is slightly Cd-leaner than $Ba_2Cd_3Bi_4$). The third structurally characterized phase in this system, the monoclinic $Ba_{11}Cd_8Bi_{14}$ is presumably a product of a peritectic reaction but small single crystals of it can also be grown from Cd-rich melts at the specified conditions [2].

2.2. Crystallographic studies

X-ray powder diffraction patterns were taken at room temperature on a Rigaku MiniFlex powder diffractometer using monochromatized Cu $K\alpha$ radiation. Samples were prepared inside a glove box by grinding crystals of $Ba_2Cd_3Bi_4$ to fine powder, placing it in a sample holder and covering the surface with a thin film of Apiezon grease. This was done with the idea to prevent the crystallites from oxidation during the data collection. The data analysis was carried out using the JADE 6.5 package. The positions of the peaks and their relative intensities matched well with those calculated from the single-crystal work.

A suitable crystal for data collection was selected in a glove box, and cut to the desired smaller dimensions ($0.10 \times 0.09 \times 0.07\,mm^3$) in Paratone N oil. The crystal, mounted on a glass fiber, was quickly placed on the goniometer of a Bruker SMART CCD-based diffractometer. After careful examination of the unit cell, data for the same crystal were collected at temperatures ranging from −173 °C to –23 °C (in 50° increments) in batch runs at different ω and ϕ angles. The procedure consists of collection of over a hemisphere of data using ω-scans with frame width of 0.5° at fixed 2θ and χ angles. The data collection was carried out using the SMART software, data integration and cell refinement were done using SAINT, respectively [6]. SADABS was used for semi-empirical absorption correction based on equivalents [7].

Inspection of the systematic absence conditions confirmed the *C*-centering of the cell and clearly suggested *Cmce* (No. 64) [8] as the most likely space group. The structure was subsequently solved by direct methods and refined by full matrix least-squares methods on F^2 using SHELXL [9]. Site occupancies were checked by freeing the site occupancy factor of an individual site, while the occupancies of the remaining sites were kept fixed, which resulted in no significant deviations from unity. Further details of the data collection and structure refinements parameters for all four data sets are given in Table 1.

In the last refinement cycles, the atomic positions were standardized using STRUCTURE TIDY [10], and all sites were refined with anisotropic displacement parameters. Final positional and equivalent isotropic displacement parameters and important bond distances from the structure refinement at −173 °C are listed in Tables 2 and 3, respectively. Anisotropic displacement parameters for the two Cd sites are given in Table 4. Further information in the form of CIF has been deposited with Fachinformationszentrum Karlsruhe, 76344 Eggenstein-Leopoldshafen, Germany, (fax: (49) 7247-808-666; e-mail: crysdata@fiz.karlsruhe.de); depository numbers CSD 416445 (−173 °C data set); CSD 416447 (−123 °C data set); CSD 416446 (−73 °C data set); CSD 416444 (−23 °C data set).

2.3. Calculations

TB-LMTO-ASA calculations were carried out by applying the LMTO-47 package [11]. This program is based on the tight-binding linear-muffin-tin orbital (LMTO) method in the local density (LDA) and atomic sphere (ASA) approximations [12]. Reciprocal space integrations are calculated by the tetrahedron method [13]. The crystal orbital hamiltonian population (COHP) method is used for the analysis of bonding interactions [14], analogous to the crystal orbital overlap population (COOP) used in the semi-empirical Hückel calculations [15]. The Fermi levels in all graphical representations are set to zero and the COHP diagrams are drawn by reversing its value with respect to the energy scale (i.e., –COHP vs. E). This is done so that the calculated peak values are negative for antibonding and positive for bonding interactions.

3. Results

3.1. Structure

As noted already, the existence of the ternary intermetallic compound $Ba_2Cd_3Bi_4$ was first reported in 1982 and its structure was determined by X-ray crystallography [4]. It crystallizes with its own type (Pearson's symbol

Table 1
Selected crystal data and structure refinement parameters for $Ba_2Cd_3Bi_4$

Empirical formula	$Ba_2Cd_3Bi_4$			
Formula weight, Z	1447.80, $Z = 4$			
Crystal system, space group	Orthorhombic, *Cmce* (No. 64)			
Temperature	−23 °C	−73 °C	−123 °C	−173 °C
Unit cell dimensions (Å)	$a = 7.019(3)$	$a = 7.015(3)$	$a = 7.009(4)$	$a = 7.001(4)$
	$b = 17.389(7)$	$b = 17.375(8)$	$b = 17.355(9)$	$b = 17.330(10)$
	$c = 9.246(3)$	$c = 9.241(4)$	$c = 9.233(5)$	$c = 9.224(6)$
Volume (Å^3)	1128.5(7)	1126.3(9)	1123.0(10)	1119.0(12)
Density (calculated, g/cm^3)	8.522	8.538	8.563	8.594
Radiation	Mo$K\alpha$, $\lambda = 0.71073$ Å			
Absorption coefficient (cm^{-1})	744.51	745.97	748.15	750.80
Reflections collected, R_{int}	3011, $R_{int} = 0.0551$	3007, $R_{int} = 0.0563$	2991, $R_{int} = 0.0541$	2979, $R_{int} = 0.0500$
Data/restraints/parameters	669/0/28	669/0/28	667/0/28	665/0/28
Final R^a indices [$I > 2\sigma_I$]	$R_1 = 0.0367$	$R_1 = 0.0381$	$R_1 = 0.0363$	$R_1 = 0.0375$
	$wR_2 = 0.0859$	$wR_2 = 0.0886$	$wR_2 = 0.0831$	$wR_2 = 0.0910$
R indices [all data]	$R_1 = 0.0460$	$R_1 = 0.0461$	$R_1 = 0.0437$	$R_1 = 0.0433$
	$wR_2 = 0.0906$	$wR_2 = 0.0921$	$wR_2 = 0.0867$	$wR_2 = 0.0938$
Goodness-of-fit on F^2	1.062	1.037	1.059	1.088
Extinction coefficient	0.00056(5)	0.00064(6)	0.00061(5)	0.00052(5)
Largest diff. peak/hole (e/Å^3)	2.545/–1.624	2.123/–1.964	2.923/–1.670	2.953/–1.933

[a] $R_1 = \Sigma||F_o|-|F_c||/\Sigma|F_o|$; $wR_2 = [\Sigma[w(F_o^2-F_c^2)^2]/\Sigma[w(F_o^2)^2]]^{1/2}$, where $w = 1/[\sigma^2F_o^2 + (AP)^2 + BP]$, and $P = (F_o^2 + 2F_c^2)/3$; A and B—weight coefficients.

Table 2
Atomic coordinates and equivalent isotropic displacement parameters for $Ba_2Cd_3Bi_4$ refined from data collected at −173 °C

Atom	Wyckoff site	x	y	z	U_{eq} (Å^2)
Ba	8*f*	0	0.1164(1)	0.4243(1)	0.0160(4)
Bi1	8*e*	1/4	0.4509(1)	1/4	0.0159(3)
Bi2	8*f*	0	0.1863(1)	0.0576(1)	0.0159(3)
Cdi	4*a*	0	0	0	0.0276(7)
Cd2	8*e*	1/4	0.2819(1)	1/4	0.0212(4)

Table 3
Selected bond distances (Å) in $Ba_2Cd_3Bi_4$ refined from data collected at −173 °C

Atom pair	Distance	Atom pair	Distance
Cd1−Bi1	3.017(1) × 4	Bi1−Cd2	2.928(3)
Cd1−Bi2	3.273(2) × 2	Bi1−Cd1	3.017(1) × 2
Cd1−Ba	4.100(2) × 4	Bi1−Ba	3.667(2) × 2
Cd2−Bi1	2.928(3)	Bi1−Ba	3.725(2) × 2
Cd2−Bi2	2.993(2) × 2	Bi2−Cd2	2.993(2) × 2
Cd2−Bi2	3.379(2) × 2	Bi2−Cd1	3.273(2)
Cd2−Ba	3.725(2) × 2	Bi2−Cd2	3.379(2) × 2
Cd2−Ba	3.897(2) × 2	Bi2−Ba	3.592(3)
		Bi2−Ba	3.633(3)
		Bi2−Ba	3.708(2) × 2

*oC*36) in the orthorhombic space group *Cmce* (No. 64) [8] and a perspective view of the structure is shown in Fig. 1. There are five atoms in the asymmetric unit, one Ba, two Cd's and two Bi's, all in special positions in *Cmce* (Table 2). Besides $Ba_2Cd_3Bi_4$, there are only a few other ternary $RE_2Al_3Ge_4$ (RE = Rare-earth metal) compounds crystallizing with that type [16], and they evidently have very different packing and electronic requirements compared to the title compound. This and the fact that the original structure refinements are with somewhat high residuals (ca. 12%) and with abnormally elongated anisotropic displacement parameters for the Cd-atoms [4], motivated us to undertake more careful examination of the crystal structure.

Table 4
Anisotropic displacement parameters in $Ba_2Cd_3Bi_4$ refined from data collected at −23 °C, −73 °C, −123 °C, and −173 °C

Atom	U_{11}	U_{22}	U_{33}	U_{13}	U_{23}	U_{33}
	−23 °C					
Cd1	0.0285(14)	0.075(2)	0.0389(19)	0.0280(17)	0.000	0.000
Cd2	0.0442(11)	0.0248(9)	0.0389(13)	0.000	−0.0153(9)	0.000
	−73 °C					
Cd1	0.0264(13)	0.065(2)	0.0311(17)	0.0223(15)	0.000	0.000
Cd2	0.0395(10)	0.0215(9)	0.0307(12)	0.000	−0.0109(8)	0.000
	−123 °C					
Cd1	0.0243(12)	0.0525(18)	0.0282(16)	0.0191(14)	0.000	0.000
Cd2	0.0327(9)	0.0202(8)	0.0265(11)	0.000	−0.0092(7)	0.000
	−173 °C					
Cd1	0.0199(12)	0.0423(16)	0.0205(15)	0.0128(12)	0.000	0.000
Cd2	0.0266(9)	0.0170(8)	0.0200(10)	0.000	−0.0062(7)	0.000

Single-crystal X-ray diffraction data collected for a flux-grown crystal at four different temperatures confirmed the formerly proposed structure and converged to excellent final residuals (Table 1). All structure refinement indicators suggest the model to be a good fit (small standard deviations, low R_{int}, featureless difference Fourier map, etc.), yet the two Cd sites exhibit slightly elongated anisotropic displacement parameters (Table 4). The quality of the crystal and the much better intensity data from the

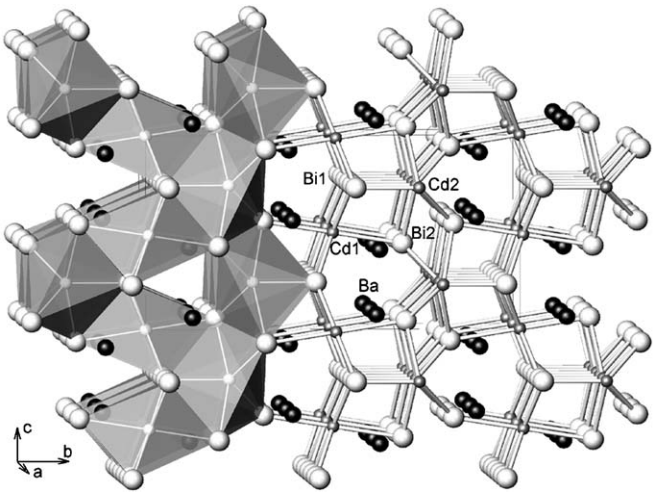

Fig. 1. A perspective view of the orthorhombic structure of $Ba_2Cd_3Bi_4$, both in polyhedral and ball-and-stick representations. Bismuth atoms are shown as large light spheres, cadmium atoms are shown as small gray spheres or as centering atoms in the shaded polyhedra, barium atoms are shown as black spheres. The unit cell and the viewing direction are denoted as well.

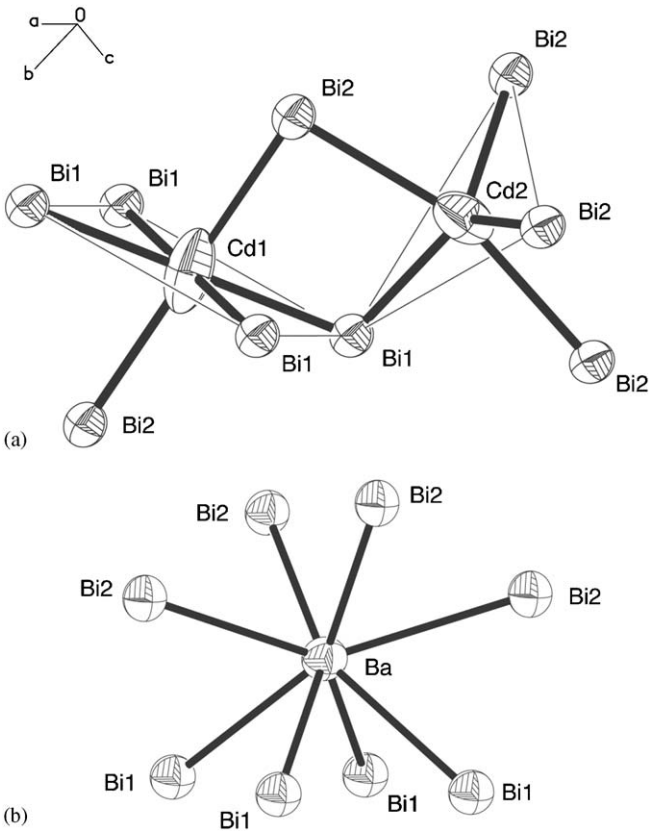

Fig. 2. Close-up view of the coordination environment around Cd1 and Cd2 (a), and around the Ba atoms (b). Anisotropic displacement parameters are drawn at the 95% probability level.

CCD-detector attribute to the low *R*-values; however, the elongation and the strong temperature dependence of the shape of the anisotropic displacement parameter of Cd1 especially (Wyckoff site 4*a*), is indicative of a small positional disorder. This unusual aspect in the structure of $Ba_2Cd_3Bi_4$ is presented graphically in Fig. 2a; the anisotropic displacement parameters for Cd1 at the four data collection temperatures are tabulated in Table 4.

It is interesting to note that Cd1 and Cd2 have unique coordination—six-coordinated elongated octahedron for Cd1 and five-coordinated trigonal bi-pyramid for Cd2 (Fig. 2, Table 3). The typical tetrahedrally coordinated Cd does not exist in this compound, whereas it is the prevailing motif in other *A*–Cd–*Pn* compounds ($A = Sr$ or Ba; $Pn = Sb$ or Bi), such as $BaCdBi_2$ [5], $Ba_{11}Cd_8Bi_{14}$ [2], $Sr_9Cd_4Bi_9$ [17], $Sr_{11}Cd_6Sb_{12}$ [18], to name just a few. Four coplanar Bi1 are equidistantly positioned around Cd1 with Cd–Bi distance of 3.017(1) Å, while the two apical Bi2 atoms are quite farther away from the Cd1, with Cd–Bi distance of 3.273(2) Å. The coordination octahedron is not only elongated in the direction of the Bi2–Cd1–Bi2 bonding, but it is also somewhat distorted along this axis—the deviation from the right angle at the base is 8.86(3)°. Similarly distorted is the trigonal bi-pyramid around Cd2—this Cd site is in the plane of three Bi atoms, two Bi2 and one Bi1, with distances ranging from 2.928(3) to 2.993(2) Å for Cd2–Bi1 and for Cd2–Bi2, respectively (Table 3), which compare well with those in $BaCdBi_2$ [5] and $Ba_{11}Cd_8Bi_{14}$ [2], for instance. The two apical Bi2 atoms are again weakly bonded with longer Cd–Bi distance of 3.377(2) Å. We note here that for both Cd1 and Cd2, the elongation of the corresponding anisotropic displacement parameters occurs in directions almost parallel to the direction of the apical bonds, which seems to indicate that the weaker coordination is the origin for such anomaly. Although the structures of the isotypic $RE_2Al_3Ge_4$ (RE = rare-earth metal) compounds [16] are refined from powder X-ray diffraction data and with isotropic displacement parameters only, the Al atom at the 4*a* site (*i.e.* the equivalent of Cd1 in $Ba_2Cd_3Bi_4$) has more than 50% larger thermal parameter than the rest [16]. This is a hint that the above-described anomaly concerning the displacement parameter of Cd1 in the structure of $Ba_2Cd_3Bi_4$ is an intrinsic feature of this family. Analysis of the integrated COHP's confirms that these bonds are substantially weaker than the rest.

Last, the three-dimensional anionic sub-network in $Ba_2Cd_3Bi_4$ is built via corner- and edge-sharing of the Cd1-centered octahedra and the Cd2-centered trigonal bi-pyramids (Fig. 1). The connectivity between these polyhedra is quite complicated: each octahedron is linked to six trigonal bi-pyramids (four by edge-sharing and two by corner-sharing) and to four additional octahedra (all by corner-sharing). The Ba cations occupy the cavities within the polyanionic framework and the coordination of the Ba atoms can be viewed as a strongly distorted square antiprism, with Bi–Ba distances ranging from 3.592(3) to 3.725(2) Å (Table 3, Fig. 2b).

3.2. Thermal expansion

To fully understand the cause for the large displacements of the Cd atoms in the structure of $Ba_2Cd_3Bi_4$, single-crystal X-ray diffraction data were collected at four different temperatures and the structure was refined accordingly. The variation of the unit cell parameters with the temperature is shown in Table 1—while the cell volume exhibits almost linear thermal expansion ($\beta \approx 5.6 \times 10^{-5} K^{-1}$),[1] the changes in the three different crystal axial directions are very different. The temperature dependence of the *b*-axis is very strong (ca. 0.35% difference), whereas it is weaker for the *a*- and the *c*-axis, ca. 0.26 and 0.24% difference, respectively. Furthermore, the corresponding changes in the bond distances with the temperature (Fig. 3) indicate that the anisotropy along the *b*-axis correlates strongly with the elongation/contraction of the apical Cd1–Bi2 bonds in the Cd1-centered octahedra, which as discussed already, almost coincide with the direction of the longest mean-square displacement for the Cd1 atoms. The structure refinements also confirm strong temperature dependence of the cadmiums' anisotropic displacement parameters (Fig. 4). This is particularly well demonstrated on the example of Cd1—as the temperature increases its thermal ellipsoid becomes "cigar-shaped", which suggests that the site could be split into two statistically occupied sites along the direction of the Cd1–Bi2 bonding. The split is very small, ca. 0.2 Å and becomes progressively smaller as the temperature decreases so that it is not possible to refine the two partially occupied sites as such. Given the weaker apical Cd1–Bi2 interaction, it is perhaps not surprising to expect larger atomic displacement parameters in this direction compared to the directions of the in-plane Cd1–Bi1 bonding. Similar "disorder" is also observed for Cd2, however, the amplitude of these atomic "vibrations" is much lower, most likely due to the tighter five-coordination. The elongation of the thermal ellipsoid is almost along the [101] direction and its shape is also strongly temperature-dependent, especially in the direction of the major axis of the ellipsoid. All of the above confirms that the anomalies in the cadmiums' anisotropic displacement parameters and the thermal anisotropy are nuances of the structure of $Ba_2Cd_3Bi_4$, which originate from the unusual cadmium coordination.

[1]The cell parameters at room temperature obtained from powder X-ray diffraction a = 7.034(1) Å, b = 17.415(2) Å, and c = 9.267(1) Å agree well with those reported by Schäfer et al. [4] from single-crystal work (a = 7.037(1) Å, b = 17.438(2) Å, and c = 9.267(1) Å), and may suggest even larger linear thermal expansion coefficient. However, we are inclined not to draw further conclusions based on these values since the temperature studies are conducted on a single-crystal diffractometer only and might be prone to systematic instrument errors.

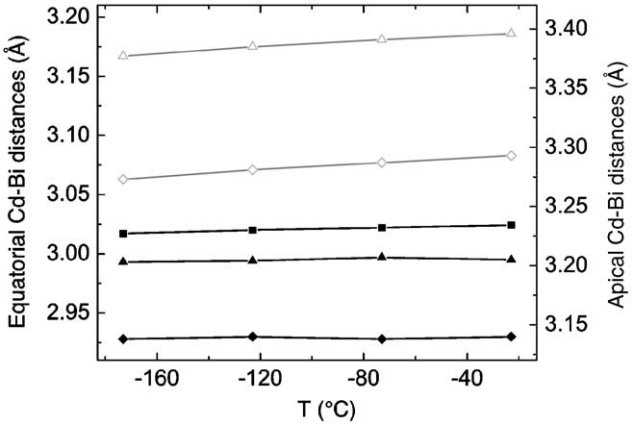

Fig. 3. Temperature dependence of the equatorial Cd–Bi (left *y*-axis) and the apical Cd–Bi (right *y*-axis) distances in $Ba_2Cd_3Bi_4$.

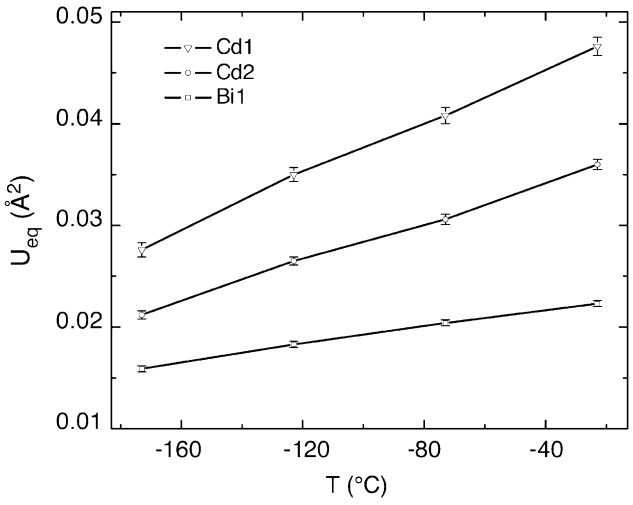

Fig. 4. Temperature dependence of the equivalent isotropic displacement parameters of Cd1, Cd2 and Bi1 in $Ba_2Cd_3Bi_4$. The behavior of the Bi2 and Ba temperature factors is virtually identical to that of Bi1 and it is not shown for clarity.

3.3. Band structure calculations

The projected DOS and the crystal orbital Hamilton population (COHP) diagrams are shown in Fig. 5. From the DOS, typical metallic bonding picture can be inferred. From the DOS for the Ba and Bi states (Fig. 5, right), it is evident that the strong bonding and antibonding regions are composed mainly of the Ba-6*s*, 6*p* and Bi-6*p* orbitals, respectively. However, the substantially populated Ba-5*d* states around the Fermi level also have an apparent contribution to the Ba–Bi bonding, and together with the Bi-6*p* states predominately contribute to the weakly bonding and antibonding regions just above the Fermi level. Due to the appreciable mixing of the latter states, the Ba–Bi bonding cannot be viewed as typical ionic-like interactions. The COHP curve for Ba–Bi interactions suggests them to be slightly electron-deficient, however,

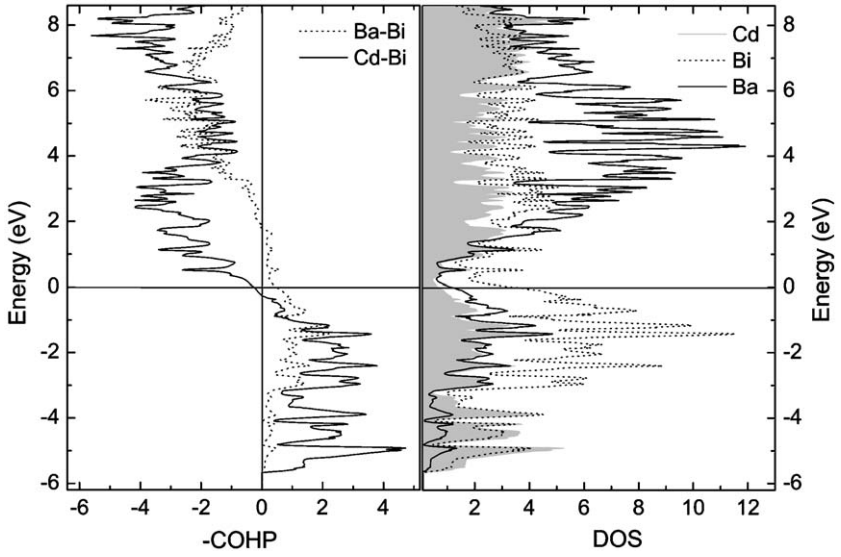

Fig. 5. COHP and Projected DOS for $Ba_2Cd_3Bi_4$. The COHP (left) for the Cd–Bi and Ba–Bi interactions are shown with solid and dashed lines, respectively. The partial DOS for Ba and Bi are also shown with solid and dashed lines, respectively, whereas the Cd DOS is represented as gray shaded area.

Table 5
Average integrated COHP values for different interactions in $Ba_2Cd_3Bi_4$

Bond	Distance	−ICOHP (eV)
Cd1−Bi1	3.017(1)	1.106
Cd1−Bi2	3.273(2)	0.570
Cd2−Bi1	2.928(3)	1.661
Cd2−Bi2	2.993(2)	1.531
Cd2−Bi2	3.379(2)	0.570
Bi1−Ba	3.667(2)	0.585
Bi1−Ba	3.725(2)	0.456
Bi1−Ba	3.592(3)	0.482
Bi1−Ba	3.633(3)	0.594
Bi1−Ba	3.708(2)	0.478

filling more electron into the Ba–Bi bands will not change much the bonding strength since the COHP curve of Ba–Bi above the Fermi level exhibits a broad area of almost nonbonding character.

For the Cd–Bi bonding, the COHP curve (Fig. 5, left) shows strong covalent character, which is mainly originated from the Cd-5*s*, 5*p* and Bi-6*p* states. Unlike the Ba–Bi interactions, the Cd–Bi bonding seem to be a bit electron excessive with a small antibonding region just below the Fermi level. Further analysis indicates that this region is originated from the interactions between the Cd's and the apical Bi's in the Cd-centered polyhedra. The average value of the integrated –COHP (Table 5), which provides quantitative comparison on the bonding strength, also suggest these contacts to be much weaker compared to the in-plane Cd–Bi ones. These results corroborate the bonding analysis based on the interpretation of the bond distances and the temperature dependence of the cadmium's anisotropic displacement parameters.

4. Conclusions

With the present work, the previously reported ternary intermetallic phase $Ba_2Cd_3Bi_4$, whose structure had been poorly characterized, was reexamined and the structure was refined at four different temperatures. The study proved the existence of a small position disorder, associated with the loosely bound Cd atoms, both having uncommon coordination–elongated octahedron and distorted trigonal bi-pyramidal, respectively. The dependence of the unit cell parameters and the shape of the anisotropic displacement parameters with the temperature are closely related to the disorder of the Cd atoms. This was further corroborated by TB-LMTO-ASA calculations, which indicate much weaker interactions along the direction of the major axis of the thermal ellipsoid.

Acknowledgments

Svilen Bobev gratefully acknowledges funding from the University of Delaware and University of Delaware Research Foundation (UDRF).

References

[1] S. Bobev, A. Lima, V. Fritsch, J.D. Thompson, J.L. Sarrao, M. Gilleßen, R. Dronskowski, Inorg. Chem. 45 (2006) 4047 published on the Web 04/15/2006.
[2] S.-Q. Xia, S. Bobev. $Ba_{11}Cd_8Bi_{14}$: Bismuth Zigzag Chains in a Ternary Alkaline-earth Transition-Metal Zintl Phase, Inorg. Chem. (2006) in print, doi:10.1021/ic060583z.
[3] S. Bobev, J.D. Thompson, J.L. Sarrao, M.M. Olmstead, H. Hope, S.M. Kauzlarich, Inorg. Chem. 43 (2004) 5044.
[4] G. Cordier, P. Woll, H. Schäfer, J. Less-Common Metals 86 (1982) 129.
[5] E. Brechtel, G. Cordier, H. Schäfer, J. Less-Common Metals 79 (1981) 131.

[6] Bruker SMART and SAINT, Bruker AXS Inc., Madison, Wisconsin, USA, 2002.
[7] G.M. Sheldrick SADABS, University of Göttingen, Germany, 2003.
[8] The space group symbol used herein *Cmce* conforms to the new symbol for double glide plane "*e*" as suggested in the 4th revised edition of the International Tables for Crystallography, The symbol for the same space group in the older literature is referred to as *Cmca*.
[9] G.M. Sheldrick SHELXTL, University of Göttingen, Germany, 2001.
[10] (a) E. Parthe, L.M. Gelato, Acta Crystallogr. 40A (1984) 169;
(b) L.M. Gelato, E. Parthe, J. Appl. Cryst. 20 (1987) 139.
[11] R.W. Tank, O. Jepsen, A. Burckhardt, O.K. Andersen, TB-LMTO-ASA Program, Version 4.7, Max-Planck-Institut Für Festkörperforschung: Stuttgart, Germany, 1998.
[12] O.K. Andersen, O. Jepsen, Phys. Rev. Lett. 53 (1984) 2571.
[13] P. Blöchl, O. Jepsen, O.K. Andersen, Phys. Rev. B 34 (1994) 16223.
[14] R. Dronskowski, P. Blöchl, J. Phys. Chem. 97 (1993) 8617.
[15] T. Hughbanks, R. Hoffmann, J. Am. Chem. Soc. 105 (1983) 3528.
[16] (a) H. Flandorfer, D. Kaczorowski, J. Gröbner, P. Rogl, R. Wouters, C. Godart, A. Kostikas, J. Solid State Chem. 177 (2004) 3418;
(b) J.T. Zhao, K. Cenzual, E. Parthe, Acta Crystallogr. 47C (1991) 1777.
[17] E. Brechtel, G. Cordier, H. Schäfer, Z. Naturforsch. 36 (9) (1981) 1099.
[18] S.-M. Park, S.-J. Kim, J. Solid State Chem. 177 (2004) 3418.